Research Article

Journal of Molecular Recognition

Received: 29 January 2014, Revised: 21 May 2014, Accepted: 27 May 2014, Published online in Wiley Online Library

(wileyonlinelibrary.com) DOI: 10.1002/jmr.2399

Force-induced globule–coil transition in laminin binding protein and its role for viral–cell membrane fusion

Boris N. Zaitsev[a], Fabrizio Benedetti[b,e], Andrey G. Mikhaylov[b], Denis V. Korneev[a], Sergey K. Sekatskii[b]*, Tanya Karakouz[b], Pavel A. Belavin[c], Nina A. Netesova[a], Elena V. Protopopova[a], Svetlana N. Konovalova[a], Giovanni Dietler[b] and Valery B. Loktev[a,d]

The specific interactions of the pairs laminin binding protein (LBP)–purified tick-borne encephalitis viral surface protein E and certain recombinant fragments of this protein, as well as West Nile viral surface protein E and certain recombinant fragments of that protein, are studied by combined methods of single-molecule dynamic force spectroscopy (SMDFS), enzyme immunoassay and optical surface waves-based biosensor measurements. The experiments were performed at neutral pH (7.4) and acid pH (5.3) conditions. The data obtained confirm the role of LBP as a cell receptor for two typical viral species of the *Flavivirus* genus. A comparison of these data with similar data obtained for another cell receptor of this family, namely human αVβ3 integrin, reveals that both these receptors are very important. Studying the specific interaction between the cell receptors in question and specially prepared monoclonal antibodies against them, we could show that both interaction sites involved in the process of virus–cell interaction remain intact at pH 5.3. At the same time, for these acid conditions characteristic for an endosome during flavivirus–cell membrane fusion, SMDFS data reveal the existence of a force-induced (effective already for forces as small as 30–70 pN) sharp globule–coil transition for LBP and LBP–fragments of protein E complexes. We argue that this conformational transformation, being an analog of abrupt first-order phase transition and having similarity with the famous Rayleigh hydrodynamic instability, might be indispensable for the flavivirus–cell membrane fusion process. Copyright © 2014 John Wiley & Sons, Ltd.

Keywords: flavivirus–cell membrane fusion; single-molecule dynamic force spectroscopy; laminin binding protein; flavivirus surface protein E; force-induced globule–coil transition

INTRODUCTION

The viral–cell membrane fusion mechanism received a lot of attention in the past, and a number of reviews in the field exist (e.g., Stiasny and Heinz, 2006; Chernomordic and Kozlov, 2008; Fritz *et al*., 2008, 2011; Harrison, 2008; Martens and McMahon, 2008; Liao *et al*., 2010; Stiasny *et al*., 2011). The fusion of two bilayer membranes is thermodynamically favorable, but there is a very high kinetic barrier. Some sufficiently effective machinery has been developed by viruses to achieve the necessary-for-infection membrane fusion. Independent of the machinery, a sufficiently large release of energy in the fusion process is required to overcome this high kinetic barrier (Harrison, 2008).

Among different kinds of membrane fusion processes, that of flaviviral–cell membrane fusion is one of the most effective and best studied. Flavivirus penetration into the cell is related with the receptor-dependent endocytosis, which implies, first, certain viral ligand–cell receptor interaction(s) and then membrane fusion, which is believed to be initiated by conformational changes of the flaviviral surface protein E taking place at low-pH conditions inside an endosome (Stiasny and Heinz, 2006; Stiasny *et al*., 2011). In an acid environment, dimers of the viral protein E are converted into trimers, and the release of a fusion peptide, its conformational transformation and interaction with the cell membrane take place. This leads to the membrane fusion and, finally, to viral RNA penetration into a cell and infection.

* *Correspondence to: Sergey K. Sekatskii, Laboratoire de Physique de la Matière Vivante, IPMC, BSP, Ecole Polytechnique Fédérale de Lausanne (EPFL), CH-1015 Lausanne, Switzerland.*
E-mail: Serguei.Sekatski@epfl.ch

a *B. N. Zaitsev, D. V. Korneev, N. A. Netesova, E. V. Protopopova, S. N. Konovalova, V. B. Loktev*
Department of Molecular Virology for Flaviviruses and Viral Hepatitis, State Research Center for Virology and Biotechnology "Vector", Koltsovo, Novosibirsk region, 630559, Russia

b *F. Benedetti, A. G. Mikhaylov, S. K. Sekatskii, T. Karakouz, G. Dietler*
Laboratoire de Physique de la Matière Vivante, IPMC, BSP, Ecole Polytechnique Fédérale de Lausanne (EPFL), CH-1015, Lausanne, Switzerland

c *P. A. Belavin*
Institute of Cytology and Genetics, Lavrentjev avenue 10, Novosibirsk 630090, Russia

d *V. B. Loktev*
Novosibirsk State University, Pirogova street 2, Novosibirsk 630090, Russia

e *F. Benedetti*
Center for Integrative Genomics, University of Lausanne, Genopode Building, CH-1015, Lausanne, Switzerland

Despite the circumstance that many details of such a process have been profoundly discussed, it is broadly accepted that the picture is still incomplete and further researches are needed. The study of the flaviviral–cell membrane fusion process can profit from the unique feature of the corresponding interaction, namely the existence of at least two different receptor–ligand interactions important for the initial stages of the virus attachment to the cell membrane and, what seems very probable, also to the membrane fusion.

The first important receptor–ligand interaction involves integrins, which are known to play the role of surface cell receptors. This proposition has been put forward after the discovery of the RGD (Arg-Gly-Asp), or RGD-like, motives in amino acid sequences of domain III of protein E of certain flaviviruses (Becker, 1990; Lobigs *et al*., 1990; van der Most *et al*., 1999). Lately, the importance of integrins for the process of flavivirus virion–cell integration has been confirmed experimentally (Chu and Ng, 2004; Lee *et al*., 2006). In particular, for the West Nile virus (WNV) surface protein E, the characteristic bond rupture force pertinent for this interaction has been estimated using the single-molecule dynamic force spectroscopy (SMDFS) method, and the possibility to use certain relatively short fragments of the surface protein E to study the corresponding receptor–ligand interaction also has been demonstrated (Bogachek *et al*., 2008, 2010).

Additionally, it has been shown that laminin binding protein (LBP; its other name is 37/67-kDa human laminin receptor) also is a cell receptor in the case of tick-borne encephalitis virus (TBEV; Protopopova *et al*., 1999). These demonstrations enabled us to propose and then to experimentally confirm the existence of an additional and different receptor region for the case of WNV protein E, the region located in the domain II of this protein and very close or identical to the location of the fusion peptide (Morozova *et al*., 2009). Specificity of the corresponding interaction with LBP has been also confirmed by the mapping of an interaction site using a C-end LBP fragment (Malygin *et al*., 2009). Note that LBP is exploited as a cell receptor also by dengue, Sindbis and Venezuelan equine encephalitis viruses (Strauss *et al*., 1994; Ludwig *et al*., 1996; Bondarenko *et al*., 2003). Similarly, it is used for this purpose also by prion proteins, and this exact circumstance is considered as the reason of LBP importance for prion-related decease pathogenesis (Gauczynski *et al*., 2001; Zuber *et al*., 2008). For completeness, we would like to mention that molecules of glycosaminoglycane, heparan sulfate and proteoglycans also might be putative cell receptors for flaviviruses (Lee and Lobigs, 2000; Chien *et al*., 2008; Okamoto *et al*., 2012).

The existence of two very distinct receptor regions in the viral protein E and anticipation that the corresponding interactions might depend differently on the pH level of the environment suggest a cycle of experiments where these specific interactions should be systematically tested at different conditions by a number of research methods. This should permit us to elucidate still unclear aspects of viral–cell membrane interaction and fusion. The first results of such experiments are reported in the present paper. We study the interaction between the full-size TBEV protein E, its recombinant fragments $E_{257–415}$ and $E_{1–254}$, as well as recombinant fragments $E_{1–180}$ and $E_{153–126}$ of WNV protein E, with their putative cell receptors, namely αVβ3 integrin and LBP, exploiting SMDFS and immunoenzyme analysis (IEA) methods. In some instances, optical surface waves-based biosensor measurements also were used to establish the efficiency of the specific interactions in question. Experiments were performed at neutral and acid pH values characteristic of the local environment of cell receptors on the surface of cells and endosome membranes.

Part of the work is closely related to our previous, also combined SMDFS–IEA, studies of receptor–ligand interactions of the WNV protein E and its fragments (Bogachek *et al*., 2008, 2010); in those papers, we already had an opportunity to underline the importance of such combined studies for the virological researches. Many results obtained now are rather similar to the previous ones. However, our current SMDFS experiments with LBP revealed what we believe is a new and unexpected phenomenon of the force-induced globule–coil transition for this protein and some of its complexes with different fragments of viral E protein. Moreover, the capability of such complexes to make a globule–coil transition was shown to be pH dependent (in almost all cases, it exists only in acid conditions), which also seems really important for understanding the membrane fusion.

This same force-induced globule–coil transition, which has been predicted by Halperin and Zhukova in 1991 and later was the subject of a number of publications, is a kind of surface tension-driven instability leading to "explosive" reorganization of a (bio)polymer in conditions of poor solvability and certain applied force. It has important similarities with celebrated Rayleigh instability in liquids (sf. Haupt *et al*., 2002). The explosive character of this process might well explain the very effective local membrane destruction necessary for the viral–cell membrane fusion. In our opinion, similar processes not only can be important for the case in question but also have much more global biological implications.

MATERIALS AND METHODS

Proteins

Tick-borne encephalitis virus, strain 205, has been cultivated onto pig embryo kidney cell culture with the subsequent purification by differential centrifugation as described by Gaïdamovich *et al*. (1990). Full-size protein E has been extracted from TBEV purified in the saccharose density gradient. To this end, viral suspension has been lysed by a buffer solution containing 20 mM TRIS–HCl, pH 7.5; 100 mM NaCl, 0.4% sodium deoxycholate (Sigma, Germany), 1% nonident P-40 (Sigma), 1 mM phenylmethylsulfonyl fluoride (Sigma), 17.5 mM EDTA with the subsequent removal of non-lysed material using a high-speed centrifuge. Additional purification of protein E has been effected by affine chromatography on the column of Sepharose containing immobilized monoclonal antibodies (mAbs) 10H10, as recommended by the BrCN-Sepharose producer.

Recombinant fragments $E_{257–415}$ and $E_{1–254}$ of the TBEV protein E, strain 205, have been constructed from viral cDNA by polymerase chain reaction method. Exactly the same recombinant fragments $E_{1–180}$ and $E_{126–153}$ of WNV protein E as in our previous research (Bogachek *et al*., 2008) were used.

Endonuclease restriction sites of *Bgl*II and *Hind*III have been inserted into primers for polymerase chain reaction, and the so-obtained fragments of cDNA have been cloned in pGSDI plasmid with the addition of a polyhistidine-tag to purify recombinant polypeptides by the affine chromatography method. Recombinant LBP has been produced and purified by metal-chelate chromatography as discussed by us before (Sorokin *et al*., 2000). mAbs to LBP and TBEV protein E have been produced as discussed by us before (Protopopova *et al*., 1996; Malygin *et al*., 2009). The

Journal of Molecular Recognition

$E_{257–415}$ and $E_{1–254}$ polypeptides and protein E of TBEV were detected by means of the IEA with mAbs 10H10 against protein E of TBEV for capturing viral antigens on the surface of 96-well polystyrene plates. Immune complexes were detected by EB1 mAb against protein E of TBEV labeled with biotin, which was revealed by avidin–peroxidase as described earlier (Ternovoi *et al*., 2007).

Human αVβ3 integrin supplied by Chemicon Corp., Billerica, MA, USA, has been used.

Enzyme immunoassay and optical surface waves-based biosensor measurements

Enzyme immunoassay was performed as described by Bogachek *et al*. (2005). Optical density was recorded at 492 nm with a Uniscan spectrophotometer, Labsystem, Helsinki, Finland.

The same label-free optical surface wave-based biosensor measurements as described in our recent paper (Konopsky *et al*., 2013) was used. Angular interrogation of the optical surface wave resonance (at a wavelength of 658 nm) was exploited to detect the thickness of the adsorbed layer, while an additional simultaneous detection of the critical angle of total internal reflection provides independent data on the liquid refraction index. It has been demonstrated that the precision and reliability of the data pertinent to receptor–ligand interprotein interactions obtained with this biosensor is quite comparable with, and in many cases even better than, that available when using somewhat similar, broadly accepted surface plasmon resonance-based detectors (e.g. Homola, 2008).

The procedure of the protein fixation onto the quartz surface of the biosensor chip and other details of experimental procedure differ insignificantly from those described by Konopsky *et al*. (2013) when discussing the experiments with rabbit and mouse immunoglobulin G (IgG) and anti-rabbit and anti-mouse IgG protein pairs. Briefly, after cleaning, the sensor chips were modified with 3-aminopropyltriethoxysilane (APTES) by 5-min immersion in a 1 vol.% APTES solution in 95% chloroform, followed by drying first under a stream of nitrogen and finally in low vacuum for 30 min. The ligand was immobilized on an amino-functionalized chip surface in the flow cell mounted to the biosensor instrument. The flow rate in all experiments was 7.5 μl/s. The ligand, in the concentration range of 15–30 μg/ml, was injected into the running buffer and circulated in the system for 20 min, the access of the ligand was washed away by phosphate-buffered saline (PBS). Next, Bovine Serum Albumin, (Sigma, Germany, lyophilized powder, ≥ 96% (agarose gel electrophoresis)) (175 μg/ml) was made to flow in the cell to block unoccupied sites and to prevent nonspecific adsorption of analyte. The interaction of analyte with the adsorbed ligand was studied at different concentrations (1–25 μg/ml). The analyte was injected into the running buffer and circulated in the system for 15 min, followed by washing with PBS. Recovery of the sensor chip was performed with 0.1 M HCl. This cycle was repeated for each analyte concentration.

Atomic force microscopy

During the previous 15–20 years, the SMDFS method achieved certain maturity, and it is rapidly becoming a more and more indispensable approach to study related problems, see reviews (e.g., Weisel *et al*., 2003; Lee *et al*., 2007; Kumar and Lee, 2010; Zhang, 2011) for the method fundamentals.

Essentially the same experimental setup and procedure of tip and sample functionalization, which have been used for the SMDFS earlier and described in detail in our papers (Chtcheglova *et al*., 2004; Bogachek *et al*., 2008, 2010; Sekatskii *et al*., 2010), were exploited for almost all protein pairs used in this study, which enables us to give here only a rather brief account. The data were obtained in Lausanne using the atomic force microscope (AFM) Nanoscope IV "Picoforce," Bruker Corp., Madison, USA. All experiments were performed using different V-shaped Si_3N_4 (silicon nitride) cantilevers (Bruker) having nominal spring constants of 0.06 and 1.2 N/m. The spring constant of each cantilever was calibrated just prior to the measurements using the built-in calibration procedure of Nanoscope IV Picoforce AFM. The typical approach–retract cycle used in these experiments for all protein pairs studied can be described as follows. The whole range of the cantilever displacement equal to 300–500 nm has been set, and the starting point has been selected in such a way that a moment of the bond breaking is observed somewhere not very far from the middle of the total displacement. For such a setting, the maximal repulsive force attained at a moment of the deepest tip–sample contact is not specially controlled and can vary in the range of 1–4 nN depending on the exact starting position of the tip and cantilever spring constant. Similarly, the time of the contact also varies depending on these parameters and approach–retract cycle repetition rate; in typical cases, it was equal to 0.1–0.2 s. Such a setting is quite standard for most SMDFS researches, and we never observed a prominent dependence of relevant experimental data on these parameters, either before or in the experiments under discussion now.

Covalent attachment of proteins onto the tip and sample surfaces without special linkers was used. Very briefly, the procedure of tip/sample functionalization was as follows. One percentage solution of glutaraldehyde (Sigma) was used as a coupling agent when functionalizing tips with viral protein E or its fragments with concentrations approximately 250 mg/l after their initial intensive cleansing. Loosely attached proteins were then removed by extensive washing with PBS buffer (for neutral pH 7.4) or citrate phosphate buffer (for pH 5.3). The protein-functionalized tips were used immediately for making measurements. Substrates (freshly cleaved muscovite mica) were functionalized for 5 min, followed by processing in a 1% v/v APTES (Sigma) solution in water. This procedure was followed by treating the substrate with a 1% v/v glutaraldehyde water solution for 15 min. After rinsing with deionized ultrahigh-quality (resistivity 18 MΩ·cm) water, the samples were immersed into a solution of LBP or integrin with a concentration of around 250 mg/l for 15 min. (In some experiments, tips were immersed into these solutions while samples were immersed into solutions of viral protein E or its fragments; this did not change the force spectroscopy data.) Non-reacted and loosely bonded proteins were subsequently removed by extensive washing with PBS or citrate phosphate buffer. Experiments were performed in these buffers for neutral and acid conditions.

The same covalent attachment of proteins onto tip and sample surfaces without special linkers has been used in our previous force spectroscopy researches with WNV protein E (or its fragments) and its putative cell receptors (Bogachek *et al*., 2008, 2010). This similarity is very important for a direct comparison of the results obtained in these aforementioned works and in the present study. We also would like to underline that our comparative researches with the "classic" SMDFS method for avidin–biotin (bovine serum albumin–biotin complex) protein pair performed using the linker-less approach presented earlier and exploiting PEG linkers, as presented for example in the site

http://www.jku.at/biophysics/content/e201852, do not reveal any material difference in the results (unpublished).

Experiments with LBP deposited onto gold plates (e.g., Sandal *et al*., 2008) and AFM tips without any protein attached have been performed in Koltsovo using Solver P47-bio AFM of NT-MDT, Moscow, Russia. The procedure of the treatment of the AFM tip was the same as described earlier, while no specific treatment has been applied to the gold support; a 10-μl droplet of LBP solution has been just deposited onto the freshly detached template-stripped gold surface, incubated for 10 min and then washed out with the buffer.

Atomic force microscopy images of mica surface functionalized in the aforementioned way demonstrate the formation of smooth protein monolayers (single molecules are seen as globules) with an average thickness of a few nanometers. Our previous single-molecule force spectroscopy studies as well as literature data attest that for the surface functionalization method and protein concentrations used, mostly single-molecule and double-molecule interactions are observed. In particular, and this was checked up again in these series of experiments, the lowering of concentration does not lead to the appearance of peaks with lower specific force in force histograms but strongly decreases the percentage of the successful approach—contract cycles, that is, such cycles where specific interaction events are recorded. For the concentrations used, the percentage of successful cycles is 20–25% for the 1000–1500 total number of cycles performed with the same cantilever/sample pair. Control experiments performed for all systems studied in conditions when one of the interacting proteins of the pair was missing (either tip or sample surfaces were not exposed to the protein solution) revealed a background noise level (force curves imitating those typical for a specific interaction) not exceeding 0.2% of cycles.

Two different software have been used to process the force spectroscopy data semiautomatically: fuzzy logic-based software by Kasas *et al*. (2000) and its newest version OpenFovea (Roduit *et al*., 2012), as well as the Hooke software (Sandal *et al*., 2009); see these original papers and that of Sekatskii *et al*. (2010) for details of the data processing. Here, we would like only to underline that these software help to filter observed bond-breaking events depending on their reliability (quality) and that the acting value of the force loading rate $\dot{F}$ is calculated by analyzing the part of the force curve observed immediately prior to the bond rupture event.

RESULTS

Interaction of the full-size TBEV protein E with putative cell receptors

The results of the SMDFS study of the interaction of full-size native TBEV protein E with LBP and αVβ3 integrin together with an example of a typical force curve are presented in Figure 1. It is clearly seen that this protein specifically (and differently) interacts with both putative receptors. For any value of the force loading rate, characteristic interaction force (bond-breaking force) for the pair protein E–LBP is materially larger than that for the pair protein E–αVβ3 integrin. Similar data have been earlier obtained by us for the protein pairs WNV protein E–LBP and WNV protein E–αVβ3 integrin, where the characteristic forces for the first pair also were systematically larger than those for the second (Bogachek *et al*., 2008, 2010).

Different slopes of the $F(\ln\dot{F})$ dependence have been observed for relatively small and relatively large force loading rates $\dot{F}$ for the pair protein E–LBP. Following the literature (see

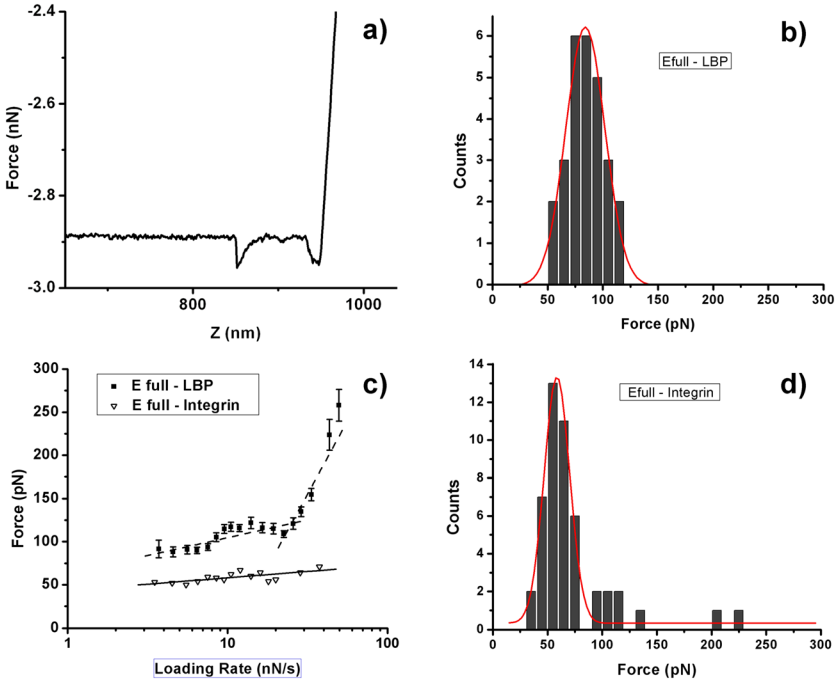

Figure 1. An example of force curve (a), single-molecule dynamic force spectroscopy data of full surface tick-borne encephalitis virus protein E–its putative cell receptors laminin binding protein (LBP) and human αVβ3–integrin interactions (c) and specific bond rupture force distribution histograms obtained for the force loading rate in the range of 8–9 nN/s (b, d).

Journal of Molecular Recognition

the aforementioned SMDFS reviews), we interpret this as an indication of existence of two different barriers/wells in the corresponding interaction landscape. Results of the analysis of the $F(\ln\dot{F})$ data, performed in the frame of a simple Bell–Evans model, $F_{prob} = (k_BT/\Delta x)\ln\dot{F} + (k_BT/\Delta x)\ln(\Delta x/k_{diss}k_BT)$ (see Evans and Ritchie, 1997, and the aforementioned SMDFS reviews), are presented in Table 1. Here, F_{prob} is the most probable bond rupture force, Δx is the barrier width, k_{diss} is the bond dissociation rate at no-force conditions, T is a temperature and k_B is a Boltzmann constant.

At the moment, we limit our analysis of the force data to the two-barrier model, excluding those models that arise because of the necessity to use more complicated bond breakage potentials (see, e.g., Dudko *et al.*, 2008; Sekatskii *et al.*, 2013, and the aforementioned SMDFS reviews). We plan to return to this question elsewhere.

Interaction of the recombinant TBEV protein E fragments $E_{1–254}$ and $E_{257–415}$ with putative cell receptors

The domain structure of protein E is known, and the similarity of the antigen structure for viral protein and its recombinant analogs has been reported earlier (Belavin *et al.*, 1997). Based on these data, two different recombinant fragments of protein E were constructed, aiming at further clarifying the location of interaction sites. The recombinant fragment $E_{1–254}$ comprises domains I and II of protein E. Polypeptide $E_{257–415}$ represents the amino acid sequence as domain III but does not comprise the transmembrane (hydrophobic, 86 aa) region.

The results of the SMDFS study of interaction of recombinant fragments of TBEV protein E with LBP and αVβ3 integrin are presented in Figure 2. The most important result obtained during the study of the interactions of these recombinant proteins with putative cell receptors is the observation of specific interactions for the pairs $E_{1–254}$–LBP and $E_{257–415}$–αVβ3 integrin together with the complete absence of such interactions for the "cross pairs" $E_{1–254}$–αVβ3 integrin and $E_{257–415}$–LBP, where the observed signal did not exceed the background level. For the first two pairs, we present the relevant experimental data on Figure 2. The kinetic parameters of the specific interactions studied are presented in Table 1. For illustration, in Figure 3, we present the energy landscape obtained for the interaction between $E_{1–254}$ and LBP.

Dependence of receptor–ligand interactions on pH level

Speaking about the dependence of receptor–ligand interactions on the pH value, we must clearly distinguish SMDFS from other methods. Let us start with SMDFS data first. In all cases except the LBP–TBEV $E_{1–254}$ and LBP–WNV $E_{1–180}$ and $E_{153–126}$ polypeptide pairs, the interactions did not depend essentially on the pH value, while for the latter, the observed force curves were qualitatively different for the case of an acid pH of 5.3 (see Figure 4 for examples of corresponding curves; pair LBP–full-size TBEV protein E has not been studied in acid conditions because of the insufficient quantity of TBEV protein E available) and a neutral pH of 7.4 where the usual picture of a specific interaction

Table 1. Kinetic parameters of the interaction of the full-size protein E and its recombinant fragments with LBP and αVβ3 integrin

Ligand–receptor	$\Delta x = k_BT/B$ (nm)	$k_{diss} = (1/B)\exp(-A/B)$ (s^{-1})	τ_{diss} (s)
LBP–protein E, initial part of the $F(\ln\dot{F})$ dependence	0.230	1.48	0.670
LBP–protein E, final part of the $F(\ln\dot{F})$ dependence	0.021	72.00	0.014
LBP–$E_{1–254}$, initial part of the $F(\ln\dot{F})$ dependence	0.150	4.10	0.200
LBP–$E_{1–254}$, final part of the $F(\ln\dot{F})$ dependence	0.017	94.00	0.010
αVβ3 integrin–protein E	0.590	0.28	3.520
Integrin–$E_{257–415}$, initial part of the $F(\ln\dot{F})$ dependence	0.300 ± 0.050	5.00 ± 3.00	0.200
Integrin–$E_{257–415}$, final part of the $F(\ln\dot{F})$ dependence	0.070 ± 0.020	53.00 ± 15.00	0.020
Integrin–$E_{257–415}$ (pH 5.3), initial part of the $F(\ln\dot{F})$ dependence	0.290 ± 0.060	1.50 ± 0.30	0.670
Integrin–$E_{257–415}$ (pH 5.3), final part of the $F(\ln\dot{F})$ dependence	0.08 ± 0.02	19.00 ± 13.00	0.050

Notation and comments: Δx, barrier width; k_{diss}, dissociation rate in the no-force conditions; LBP, laminin binding protein; $\tau_{diss} = 1/k_{diss}$. Unless otherwise stated, pH = 7.4. Force spectroscopy data $F(\ln\dot{F})$ are approached with a straight line $F = B\ln\dot{F} + A$. Experimental errors are in all cases similar to those observed for the case of an interaction integrin–$E_{257–415}$ and presented in the table.

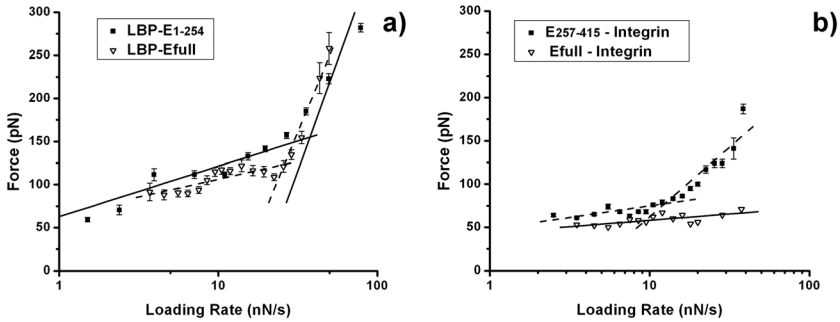

Figure 2. Single-molecule dynamic force spectroscopy data of full surface tick-borne encephalitis virus protein E and its fragments with laminin binding protein (LBP) (left) and human αVβ3 integrin (right).

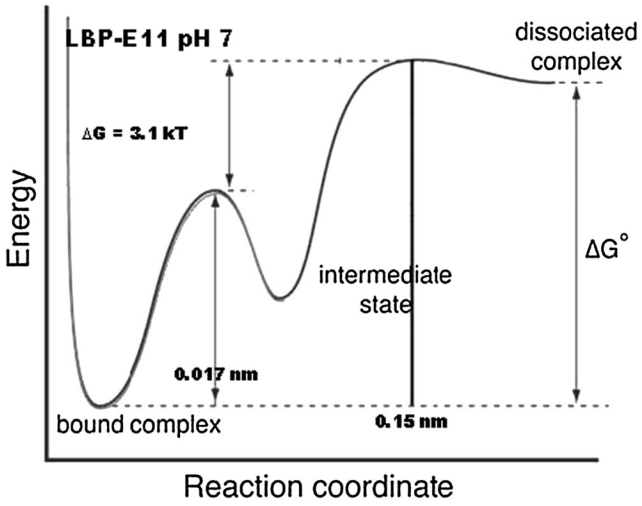

Figure 3. A model energy landscape of the laminin binding protein–E_{1-254} interaction.

characterized by an appropriate double well/barrier model has been observed. For the case of acid pH values, rather unusual "flat" force curves were observed, where the gradual increase of the stretching force before the bond breaking is lacking. The very character of these curves makes the extraction of kinetic parameters of interaction (if any) impossible.

The force spectroscopy and IEA experiments with mAbs recognizing the interaction sites of TBEV E protein (mAb 10H10; Protopopova *et al.*, 1996) and LBP (mAb 8E4; Malygin *et al.*, 2009) enable the estimate of the pH-induced changes of the interaction sites themselves. The results of these experiments are presented in Figure 5 and Table 2. No essential differences for the cases of neutral and acid pH levels were revealed for the case of the viral protein E, and only rather slight changes were noticed for LBP.

In the case of LBP–TBEV E_{1-254} interaction, its efficiency at pH 5.3 has been confirmed by another method, namely that of measurements of a photonic crystal biosensor based on optical surface waves; see Materials and Methods section for details.

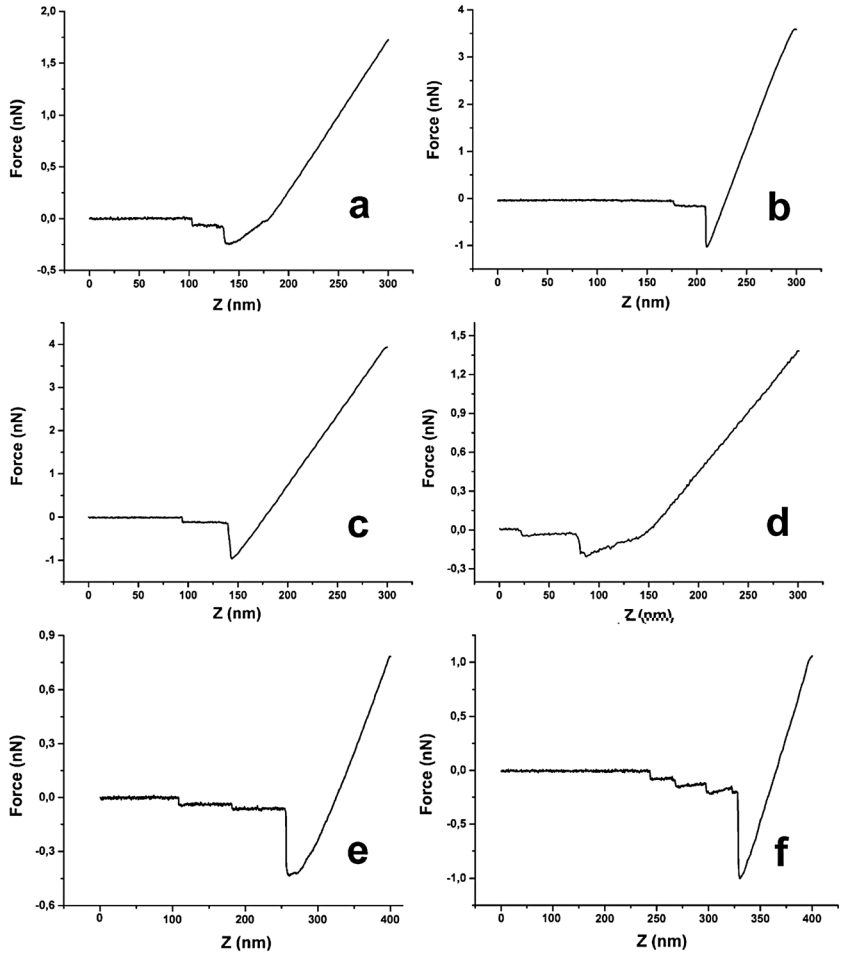

Figure 4. Examples of force curves exhibiting plateau(s) in the value of the force ("flat force curves"). (a) Laminin binding protein (LBP)–E_{1-180} protein pair of West Nile virus (WNV) at pH 5.3, (b) LBP–E_{53-126} protein pair of WNV at pH 5.3, (c) LBP deposited onto mica surface–atomic force microscopy (AFM) tip without any protein attached at pH 5.3, (d) LBP freely deposited onto freshly detached template-stripped gold surface (all other graphs present results obtained on mica surface)–AFM tip without any protein attached at pH 5.3 (curve recorded using Solver P47 Bio AFM, NT-MDT), (e) LBP–E_{1-180} protein pair of tick-borne encephalitis virus at pH 5.3 (two force plateaus are seen), (f) LBP deposited onto mica surface–AFM tip without any protein attached at pH 7.4 (three force plateaus are seen).

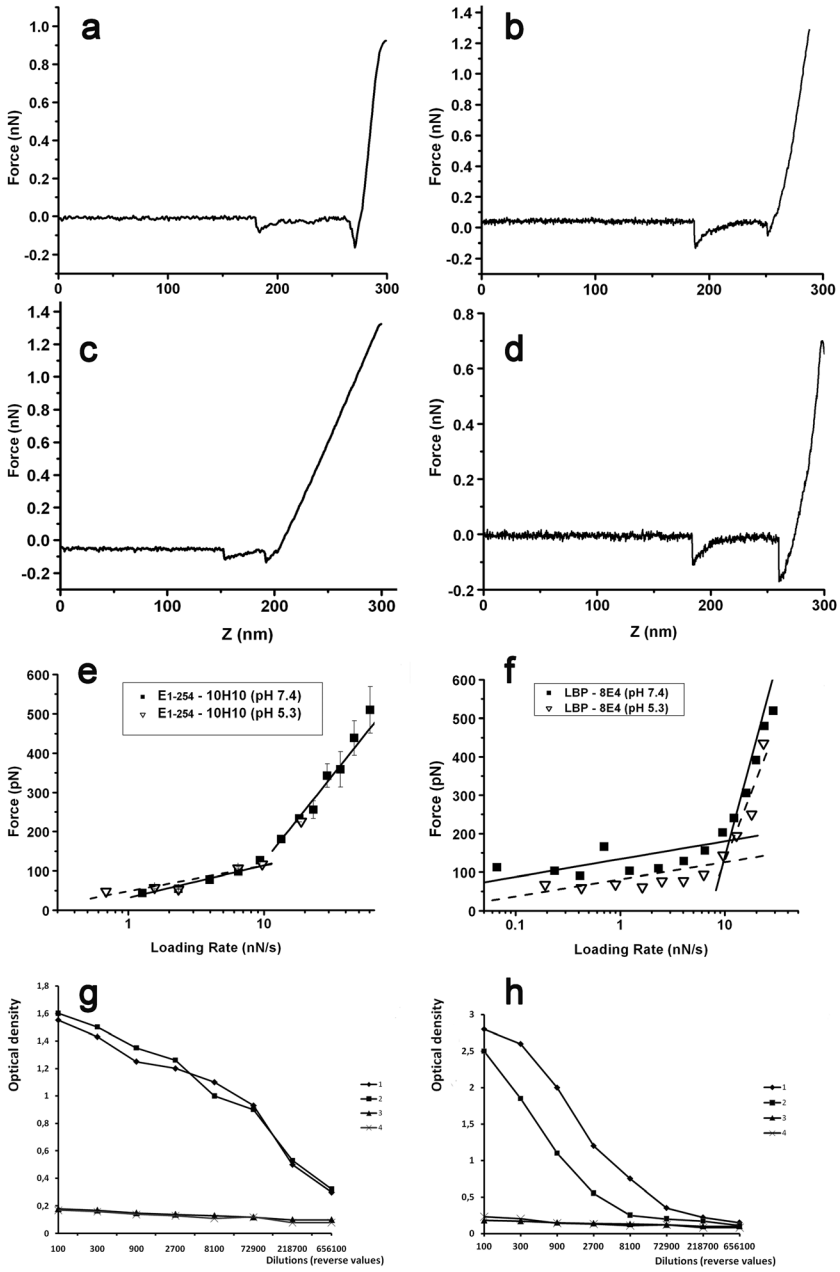

Figure 5. (a, b) Examples of force curves in the protein pairs E11–monoclonal antibodies (mAbs) 10H10 (a) and laminin binding protein (LBP)–mAbs 8E4 (b) at pH 7.4. (c, d) Examples of force curves for the same protein pairs as in (a) and (b), respectively, but at pH 5.3. (e, f) Single-molecule dynamic force spectroscopy data for interactions between antireceptor mAbs 10H10 and 8E4 and their complementary receptor regions in LBP and tick-borne encephalitis virus (TBEV) protein E molecules. (g, h) Corresponding immunoenzyme analysis data. Left, 1—interaction of 10H10 mAb with recombinant protein E_{1-254} of TBEV, pH 7.4; 2—interaction of 10H10 mAb with recombinant protein E_{1-254} of TBEV, pH 5.3; 3—interaction of 10H10 mAb with *Escherichia coli* lysate transformed by empty PQE plasmid, pH 7.4 (negative control); 4—interaction of 10H10 mAb with *E. coli* lysate transformed by empty PQE plasmid, pH 5.3 (negative control). Right: 1—interaction of 8E4 mAb with recombinant protein LBP, pH 7.4; 2—interaction of 8E4 mAb with recombinant protein LBP, pH 5.3; 3—interaction of 8E4 mAb with *E. coli* lysate transformed by empty PQE plasmid, pH 7.4 (negative control); 4—interaction of 8E4 mAb with *E. coli* lysate transformed by empty PQE plasmid, pH 5.3 (negative control).

The quantity of proteins at our disposal was not enough to extract the exact kinetic parameters of the interaction in question, but the specific interaction has been very convincingly seen when using this device, and its efficiency for different pH levels was comparable. Exact kinetic data have been obtained with this same biosensor for interactions of LBP with its mAbs; these results will be published elsewhere.

Force-induced globule–coil transitions in LBP and its complexes with fragments of the viral protein E

"Flat" force curves analogous to those presented in Figure 4 have been observed for protein pairs LBP–TBEV E_{1-254} and LBP–WNV E_{1-180} at pH 5.3. For these two pairs, "standard" force curves of the type presented in Figure 1 were never observed (i.e., were

Table 2. Kinetic parameters of the interaction of the E_{1-254} fragment of tick-borne encephalitis virus protein with 10H10 monoclonal antibody and laminin binding protein (LBP) with 8E4 monoclonal antibodies obtained at different pH levels

Ligand–receptor	$\Delta x = k_B T/B$ (nm)	$k_{diss} = (1/B)\exp(-A/B)$ (s^{-1})	τ_{diss} (s)
E_{1-254}–10H10, initial part of the $F(\ln\dot{F})$ dependence	0.120	11.000	0.087
E_{1-254}–10H10, final part of the $F(\ln\dot{F})$ dependence	0.022	27.000	0.036
E_{1-254}–10H10, initial part of the $F(\ln\dot{F})$ dependence, pH = 5.3	0.140	6.400	0.160
E_{1-254}–10H10, final part of the $F(\ln\dot{F})$ dependence, pH = 5.3	NA	NA	NA
LBP–8E4, initial part of the $F(\ln\dot{F})$ dependence	0.207	0.062	16.200
LBP–8E4, final part of the $F(\ln\dot{F})$ dependence	0.010	16.500	0.060
LBP–8E4, initial part of the $F(\ln\dot{F})$ dependence, pH = 5.3	0.310	0.140	7.200

Notation is the same as in Table 1. Unless otherwise stated, pH = 7.4. NA, not available.

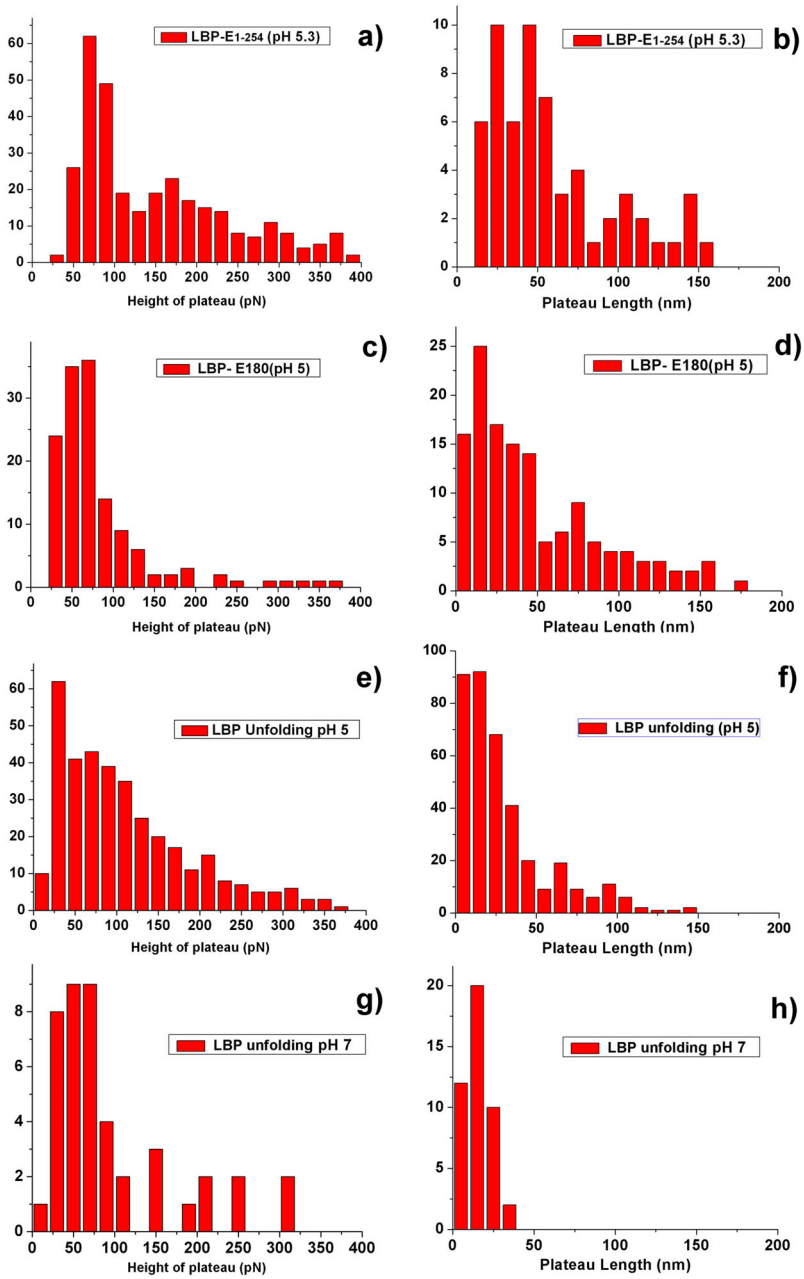

Figure 6. Histograms of the distributions of characteristic forces (force plateau heights; a, c, e, g) and force plateau lengths (b, d, f, h) observed in single-molecule dynamic force spectroscopy experiments with the protein pairs laminin binding protein (LBP)–TBEV E_{1-254} (pH 5.3), LBP–West Nile virus E_{1-180} (pH 5.3) and pure LBP (pH 5.3 and pH 7.4).

observed at the noise level). The situation for the pair LBP–WNV $E_{153–126}$ at pH 5.3 was more complicated: in most cases, standard force curves, attesting specific interaction with the parameters close to those observed at pH 7.4 (Bogachek *et al*., 2008) were recorded, but in approximately 5% of all retraction curves, small, in both the length and force values, force plateaus in the force curves were recorded.

No force curves with force plateaus have been observed for these protein pairs at pH 7.4, and no such curves have been observed for all investigated protein pairs at both pH values if there was no LBP in a protein pair. This unambiguously attests the fact that such flat force curves are associated with some peculiarities in the behavior of LBP. To elucidate this question further, we performed experiments with only LBP deposited onto the mica surface, while the AFM tip has been functionalized exactly as discussed in the Atomic Force Microscopy section, but without the last stage of adding a protein. So we had a protein-free tip capable of effectively attaching a protein on the substrate. Note that such an approach when no protein is attached to the properly modified AFM tip is quite routinely used in force spectroscopy researches, for example, when polysaccharides are studied. See also Beyer and Clausen-Schaumann (2004, and references therein) where the possibility of "mechanically assisted" formation of covalent bonds has been profoundly discussed. For such a case, flat force curves have been regularly observed for both pH levels, and no curves demonstrating a gradual increase of the force necessary to stretch proteins, characteristic of typical experiments where specific interaction is studied, were recorded. In some cases, not one but two to three or even more force plateaus in the force curves were recorded (see Figure 4 for examples).

To exclude the interpretation of the observed phenomenon as being due to the decisive influence of the LBP–support surface interaction, additional experiments with LBP freely (that is without any surface treatment) deposited onto freshly detached template-stripped gold surface (Materials and Methods section) were undertaken at pH 5.3. They revealed quite similar "flat force curves" observed in ~20% of all approach–retract cycles studied (see again Figure 4).

Experimentally observed parameters characterizing this type of force curves are given in the histograms in Figure 6. Note the presence of a number of rather well-distinguished force peaks (force plateau heights) with the period of 70–80 nm and force plateau length peaks with the period of 25 nm for the LBP–TBEV $E_{1–254}$ pair at pH 5.3. Such discretized force plateau heights and lengths were less observable for the LBP–WNV $E_{1–180}$ protein pair and unobservable for LBP stretching events.

DISCUSSION AND CONCLUSIONS

LBP as a cell receptor for TBEV and WNV

Earlier, we have already measured interactions of LBP and αVβ3 integrin with the WNV E protein using combined SMDFS and IEA approaches (Bogachek *et al*., 2008, 2010). The specificity of the corresponding interactions has been established, and the characteristic bond-breaking forces have been measured to be equal (at a force loading rate of 10 nN/s) to 105 and 210 pN, respectively, for single and double bonds for the pair LBP–WNV protein E and (for the same force loading rate) to 80 and 140 pN for such single and double bonds in the pair αVβ3 integrin–WNV protein E. This again confirms the existence of two different cell receptors for the WNV protein E. The interaction site responsible for interaction with LBP is located in the region of the fusion peptide of protein E (Morozova *et al*., 2009), while that responsible for interaction with αVβ3 integrin is usually associated with the presence of the RGD motive in domain III of protein E.

The first conclusion of the present research is the unambiguous confirmation of the existence of these two receptors also for the TBEV protein E, that is, an envelope protein of another representative of flaviviruses. The measured characteristic interaction forces turned out to be somewhat smaller than those reported for the WNV protein E, but the general similarity of the results is quite certain. This attests a known functional similarity of the interaction sites of protein E of the TBEV and WNV. Note also that for both viral proteins E, corresponding recombinant fragments still demonstrate the capability of specific interaction.

Role of LBP in viral–cell membrane fusion

The acid environment is a prerequisite of viral penetration into cell, so it is important to analyze the stability of the receptor–ligand interactions in conditions of different pH levels. All data presented earlier attest that at both neutral and acid pH conditions, specific interactions involving LBP persist, and consequently, the conformations of corresponding interaction sites remain intact or change only insignificantly. No essential dependence on the pH level has been revealed by all methods used, that is, SMDFS (where these data were available), IEA and photonic crystal biosensor based on optical surface wave data. At the same time, the SMDFS method shows a profound change of the conformational structure of LBP molecule–other protein complexes at low pH levels and attests to their transformation from a globular conformation to another much more stretched conformation with the simultaneous conservation (or "almost conservation") of the structure and interaction capabilities of the active receptor sites of the proteins involved.

What is a plausible explanation of flat force curves observed for pure LBP and LBP with other protein complexes in our experiments? Analysis of the literature data suggests proposing that we have a case of force-induced globule–coil transition of these species. Such a phenomenon has been first indicated by Halperin and Zhulina (1991) and then has been a subject of a number of theoretical or numerical (e.g., Kreitmeier *et al*., 1999; Cooke and Williams, 2003; Polotsky *et al*., 2011) and experimental publications (Haupt *et al*., 2002; Gunari *et al*., 2007). The physical essence of this phenomenon is that under weak extension (under the action of relatively small force), some globules in conditions of poor solvability can deform first into an elliptical (and may be also cylindrical) shape structure and then, at a certain critical extension, undergo a sharp transition into a "ball–string" configuration (whence globule–coil transition). Such a transition reflects an instability of the protein structure in conditions when a certain force is applied; it is driven by the surface tension and thus evidently, as was noted by Haupt *et al*. (2002), has a lot in common with Rayleigh instability of a column of liquid that undergoes a sharp transition into a series of droplets (Rayleigh Lord, 1879). The phenomenon is complex and crucially dependent on solubility conditions, as follows from theoretical analysis

and as was observed by (Gunari *et al*., 2007) for polystyrene chains in toluene and water.

In our case, we observe a similar phenomenon that crucially depends on pH level and exact protein complex composition; certainly, both these factors are very important for protein solubility. At the moment, we are not in a position to propose a detailed consideration of these aspects, which requires a large number of experimental and theoretical physical–chemical studies. Still it deserves to be mentioned that major conformational changes of LBP were hypothesized to explain its binding to laminin (Fatehullah *et al*., 2009) and are predicted (for some parts of the molecule) by molecular dynamic simulations (Di Giovanni *et al*., 2012). The most essential is, in our opinion, the very fact of the unambiguous observation of globule–coil transition involving LBP as well as the circumstance that the critical force, at which the transition takes place in most cases (Figure 6), is small enough, namely approximately 50–70 pN, and in some instances even twice smaller. Such a force can easily be achieved in the real process of viral–cell interaction, for example, being associated with the jackknife reorganization of the corresponding fusion protein claimed to be well established (Stiasny *et al*., 2011). Or maybe it is enough to note that, for example, the typical surface tension force characteristic for a circle of radius r of 1 nm is already about $F \cong 2\pi r\gamma \cong 400$ pN if one assumes for the acting surface tension the value characteristic for the water at room temperature, $\gamma \cong 0.07$ N/m.

We must say that somewhat similar flat force curves have been observed and explained quite differently also in some other works. While the case of the detachment of certain subunits from amyloid fibrils (Kellermayer *et al*., 2005; we also recently observed a similar behavior for alpha-synuclein (proto) filaments) certainly does not fit into the present context, the flat force curves observed for the case of the detachment of certain silk proteins from hydrophobic surface (Horinek *et al*., 2008), which was explained by a complex interplay of intrapeptide, surface and solvation interactions, cannot be so easily discerned. But earlier, we already underlined that to exclude this interpretation, we have specially studied the stretching of LBP molecules freely deposited onto a freshly cleaved gold surface with a bare AFM tip, and quite similar flat force curves also have been recorded for the case.

Force spectroscopy data attest that in the course of an abrupt transition, the end-to-end distance of a molecule or molecular complex can be enlarged up to 10–20 nm or more, in some cases much more. X-ray structural studies of the LBP molecule precursor show that this protein possesses a well-defined globular structure without stabilizing covalent bonds (Jamieson *et al*., 2008), and thus, this molecule indeed potentially might be subject to so essential conformational changes. A rough estimation for this protein having a molecular weight of 43 kDa (Sorokin *et al*., 2000), made using the broadly accepted average amino acid molecular weight of 110 Da and its average length of 0.34 nm, shows that elongations as large as ~130 nm are possible.

Quite on the contrary, domains I and II of protein E are stabilized by five disulfide bonds, two of which are located directly in the receptor region of the fusion peptide (Rey *et al*., 1995). X-ray structural studies of the protein E molecule reveal that all active sites of this molecule, namely those of domains I and II interacting with LBP and that of domain III interacting with integrin, are located in distal areas of the protein (Stiasny *et al*., 2004; Luca *et al*., 2012). Native protein E is presented on the viral particle surface in the form of a dimer being organized according to the head-to-tail and tail-to-head model. In other words, this means that the domain I of one polypeptide is very close to the domain III of another polypeptide, and correspondingly, both receptor sites (those for LBP and integrin molecules) are very close to each other. At acid conditions, trimers of protein E are formed in such a manner that epitopes of domain I, including the fusion peptide, are grouped together while domain III becomes maximally distant from this region. Correspondingly, receptors for LBP and integrin also become distant. The distance between them should be of the order of the length of the protein E molecule (its trimeric form), which can be estimated as ~10 nm.

Based on these observations, we propose the following model. Some (initially small) opening in the endosome membrane (does it appear as a result of certain fusion peptide reorganization?) causes local changes of the pH level and exerts a large enough force onto protein complexes comprising LBP molecules, and this leads to an abrupt globule–coil transition. Such a rapid, one may say explosion-like, process could essentially enlarge the size of a primary endosome membrane opening that would lead to the penetration of viral RNA into the cell cytoplasm.

Certainly, not all details are clear yet, and additional experiments are needed to clarify and unequivocally justify the aforementioned model. In particular, we cannot combine in all details the aforementioned picture with the earlier discussed, and confirmed in many aspects, molecular model of flaviviral–cell membrane fusion developed by Stiasny *et al*. (see references given earlier). In our opinion, both these mechanisms might (and should) work cooperatively. What seems the most important for us is that there is a clear indication of the mechanism of creation of a sufficiently large defect in the membrane (or we may speak about a partial membrane rupture); an indication that we believe was lacking before. Let us remind again that fusion of two bilayer membranes is thermodynamically favorable, but there is a very high kinetic barrier to be overcome (Chernomordic and Kozlov, 2008; Harrison, 2008), and the creation of a large enough defect in an initially intact membrane does appear as an effective way to do this.

Briefly, we can summarize the role of the LBP molecule during a membrane fusion process as follows: at least, this molecule ensures *a non-rigid flexible* (capable of essential spatial changes) fixation of a viral particle onto the endosome membrane, or as proposed earlier, LBP also could work as *the main motor for creation of large enough membrane defects*, thus ensuring the subsequent membrane fusion and penetration of viral RNA into an endosome. More generally, we believe that similar processes of abrupt globule–coil transformation might occur frequently in different biological systems and have important implications in numerous life processes and, consequently, also for elaboration of antiviral drugs.

Acknowledgements

This work has been supported in part by grants of the President of the Russian Federation no. SSc-65387.2010.4 and no. SSc-2996.2012.4, Russian Foundation of Basic Researches grant 12-04-00563-a, Russian Federal contracts FC no. 53-d and FC 14.741.12.0366 and the Swiss National Science Foundation grant nos. 200020-149424 and 200021-150161.

Journal of Molecular Recognition

REFERENCES

Becker Y. 1990. Computer analysis of antigenic domains and RGD-like sequences (RGWG) in the E glycoprotein of flaviviruses: an approach to vaccine development. *Virus Genes* **4**: 267–282.

Belavin PA, Netesova NA, Reshetnikov CC, Ivanisenko VA, Eroshkin AM, Protopopova EV, Loktev VB, Malygin EG. 1997. Expression of Japanese encephalitis virus gene E fragments in *Escherichia coli* cells. *Biotechnol* **3**: 3–9, in Russian.

Beyer MK, Clausen-Schaumann H. 2004. Mechanochemistry: the mechanical activation of covalent bonds. *Chem. Rev.* **105**: 2921–2948.

Bogachek MV, Protopopova EL, Ternovoi VA, Kachko AV, Ivanova AV, Ivanisenko VA, Loktev VB. 2005. Immunochemical properties of recombinant polypeptides mimicking domains I and II of West Nile virus glycoprotein E. *Mol. Biol. (Moscow).* **39**: 710–718.

Bogachek MV, Protopopova EV, Loktev VB, Zaitsev BN, Favre M, Sekatskii SK, Dietler G. 2008. Immunochemical and single molecule force spectroscopy studies of specific interaction between the laminin binding protein and the West Nile virus surface glycoprotein E domain II. *J. Mol. Recognit.* **21**: 55–62.

Bogachek MV, Zaitsev BN, Sekatskii SK, Protopopova EV, Ternovoi VA, Ivanova AV, Kachko AV, Ivanisenko VA, Dietler G, Loktev VB. 2010. Characterization glycoprotein E C-end of West Nile virus and evaluation of its interaction force with αVβ3 integrin as putative cellular receptor. *Biochem. (Moscow).* **75**: 472–480.

Bondarenko EI, Protopopova EV, Konovalova SN, Sorokin AV, Kachko AV, Surovtsev IV, Loktev VB. 2003. Laminin-binding protein (LBP) as a cellular receptor for the virus of Venezuelan equine encephalomyelitis (VEE): part 1. A study of the interaction between VEE virus virions and the human recombinant LBP. *Mol. Gen. Mikrobiol. Virusol.* **4**: 36–39, in Russian.

Chernomordic LV, Kozlov MM. 2008. Mechanics of membrane fusion. *Nat. Struct. Mol. Biol.* **15**: 675–683.

Chien YJ, Chen WJ, Hsu WL, Chiou SS. 2008. Bovine lactoferrin inhibits Japanese encephalitis virus by binding to heparan sulfate and receptor for low density lipoprotein. *Virology* **379**: 143–151.

Chtcheglova LA, Shubeita GT, Sekatskii SK, Dietler G. 2004. Force spectroscopy with a small dithering of AFM tip: a method of direct and continuous measurement of the spring constant of single molecules and molecular complexes. *Biophys. J.* **86**: 1177–1184.

Chu JJ, Ng ML. 2004. Interaction of West Nile virus with alpha v beta 3 integrin mediates virus entry into cells. *J. Biol. Chem.* **279**: 54533–54541.

Cooke IR, Williams DRM. 2003. Stretching polymers in poor and bad solvents: pullout peaks and an unraveling transition. *Europhys. Lett.* **64**: 267–273.

Di Giovanni C, Grottesi A, Lavecchia A. 2012. Conformational switch of a flexible loop in human laminin receptor determines laminin-1 interaction. *Eur. Biophys. J.* **41**: 353–358.

Dudko OK, Hummer G, Szabo A. 2008. Theory, analysis, and interpretation of single-molecule force spectroscopy experiments. *Proc. Natl. Acad. Sci. U. S. A.* **105**: 15755–15760.

Evans E, Ritchie K. 1997. Dynamic strength of molecular adhesion bonds. *Biophys. J.* **73**: 1541–1555.

Fatehullah A, Doherty C, Pivato G, Allen G, Devine L, Nelson J, Timson DJ. 2009. Interactions of the 67 kDa laminin receptor and its precursor with laminin. *Biosci. Rep.* **30**: 73–79.

Fritz R, Stiasny K, Heinz FX. 2008. Identification of specific histidines as pH sensors in flavivirus membrane fusion. *J. Cell Biol.* **183**: 353–361.

Fritz R, Blazevic J, Taucher C, Pangerl K, Heinz FX, Stiasny K. 2011. The unique transmembrane hairpin of flavivirus fusion protein E is essential for membrane fusion. *J. Virol.* **85**: 4377–4385.

Gaĭdamovich SI, Loktev VB, Lavrova NA, Maksiutov AZ, Mel'nikova EE, Pereboev AV, Protopopov EV, Razumov IA, Sveshnikova NA, Khusainova AD. 1990. Monoclonal antibodies cross-reacting with the tick-borne encephalitis virus and with the Venezuelan equine encephalomyelitis virus. *Vopr. Virusol.* **35**: 221–225, in Russian

Gauczynski S, Peyrin JM, Haïk S, Leucht C, Hundt C, Rieger R, Krasemann S, Deslys JP, Dormont D, Lasmézas CI, Weiss S. 2001. The 37-kDa/67-kDa laminin receptor acts as the cell-surface receptor for the cellular prion protein. *EMBO J.* **20**: 5863–5875.

Gunari N, Balazs A, Walker GC. 2007. Force-induced globule–coil transition in single polystyrene chains in water. *J. Am. Chem. Soc.* **129**: 10046–10047.

Halperin A, Zhulina EB. 1991. On the deformation behavior of collapsed polymers. *Europhys. Lett.* **15**: 417–421.

Harrison SC. 2008. Viral membrane fusion. *Nat. Struct. Mol. Biol.* **15**: 690–698.

Haupt BJ, Senden TJ, Sevick EM. 2002. AFM evidence of Rayleigh instability in single polymer chains. *Langmuir* **18**: 2174–2182.

Homola J. 2008. Surface plasmon resonance sensors for detection of chemical and biological species. *Chem. Rev.* **108**: 462–478.

Horinek D, Serr A, Geisler M, Pirzer T, Slotta U, Lud SQ, Garrido JA, Scheibel T, Hugel T, Netz RR. 2008. Peptide adsorption on a hydrophobic surface results from an interplay of solvation, surface, and intrapeptide forces. *Proc. Natl. Acad. Sci. U. S. A.* **105**: 2842–2847.

Jamieson KV, Wu J, Hubbard SR, Meruelo D. 2008. Crystal structure of the human laminin receptor precursor. *J. Biol. Chem.* **283**: 3002–3005.

Kasas S, Riederer BM, Catsicas S, Cappella B, Dietler G. 2000. Fuzzy logic algorithm to extract specific interaction forces from atomic force microscopy data. *Rev. Sci. Instrum.***71**: 2082–2086.

Kellermayer MSZ, Grama L, Karsai A, Nagy A, Kahn A, Datki ZS, Penke B. 2005. Reversible mechanical unzipping of amyloid β-fibrils. *J. Biol. Chem.* **280**: 8464–8470.

Konopsky VN, Karakouz T, Alieva EV, Vicario C, Sekatskii SK, Dietler G. 2013. Photonic crystal biosensor based on optical surface waves. *Sensors.* **13**: 2566–2578.

Kreitmeier S, Wittkop M, Göritz D. 1999. Computer simulations on the cyclic deformation of a single polymer chain above and below the Θ temperature. *Phys. Rev. E.* **59**: 1982–1988.

Kumar S, Lee MS. 2010. Biomolecules under mechanical force. *Phys. Rep.* **486**: 1–74.

Lee CK, Wang YM, Huang LS, Lin S. 2007. Atomic force microscopy: determination of unbinding force, off rate and energy barrier for protein–ligand interaction. *Micron* **38**: 446–461.

Lee E, Lobigs M. 2000. Substitutions at the putative receptor-binding site of an encephalitic flavivirus alter virulence and host cell tropism and reveal a role for glycosaminoglycans in entry. *J. Virol.* **74**: 8867–8875.

Lee JW, Chu JJ, Ng ML. 2006. Quantifying the specific binding between West Nile virus envelope domain III protein and the cellular receptor αVβ3 integrin. *J. Biol. Chem.* **281**: 1352–1360.

Liao M, Sánchez-San Martín C, Zheng A, Kielian M. 2010. In vitro reconstitution reveals key intermediate states of trimer formation by the dengue virus membrane fusion protein. *J. Virol.* **84**: 5730–5740.

Lobigs M, Usha R, Nestorowicz A, Marshall ID, Weir RC, Dalgarno L. 1990. Host cell selection of Murray Valley encephalitis virus variants altered at an RGD sequence in the envelope protein and in mouse virulence. *Virology* **176**: 587–595.

Luca VC, Abi Mansour J, Nelson CA, Fremont DH. 2012. Crystal structure of the Japanese encephalitis virus envelope protein. *J. Virol.* **86**: 2337–2346.

Ludwig GV, Kondig JP, Smith JF. 1996. A putative receptor for Venezuelan equine encephalitis virus from mosquito cells. *J. Virol.* **70**: 5592–5599.

Malygin AA, Bondarenko EI, Ivanisenko VA, Protopopova EV, Karpova GG, Loktev VB. 2009. C-terminal fragment of human laminin-binding protein contains a receptor domain for Venezuelan equine encephalitis and tick-borne encephalitis viruses. *Biochem. (Moscow).* **74**: 1328–1336.

Martens S, McMahon HT. 2008. Mechanisms of membrane fusion: disparate players and common principles. *Nat. Rev. Mol. Cell Biol.* **9**: 543–556.

Morozova OV, Bakhvalova VN, Matveev LE, Shevtsova AS, Isaeva EI, Zlobin VI, Protopopova EV, Seligman S. 2009. Antigenic and immunogenic properties of multiple antigenic peptides (MAP) including flavivirus fusion peptide. *Epid. Vacc. Prevention (in Russian)* **49**: 44–50.

Okamoto K, Kinoshita H, Parquet Mdel C, Raekiansyah M, Kimura D, Yui K, Islam MA, Hasebe F, Morita K. 2012. Dengue virus strain DEN2 16681 utilizes a specific glycochain of syndecan-2 proteoglycan as a receptor. *J. Gen. Virol.* **93**: 761–770.

Polotsky AA, Smolyakova EE, Birshtein TM. 2011. Theory of mechanical unfolding of homopolymer globule: all-or-none transition on force-clamp mode vs phase coexistence in position-clamp mode. *Macromolecules* **44**: 8270–8283.

Protopopova EV, Khusainova AD, Konovalova SN, Loktev VB. 1996. Preparation and study of properties of anti-idiotypic antibodies, carrying hemagglutinating paratopes of tick-borne encephalitis virus on their surface. *Vopr. Virusol.* **41**: 50–53, in Russian

Protopopova E, Sorokin A, Konovalova S, Kachko A, Netesov S, Loktev V. 1999. Human laminin binding protein as a candidate in cell

receptor for the tick-borne encephalitis virus. *Zenr. bl. Bacteriol.* **289**: 632–638.
Rayleigh Lord SRF. 1879. On the stability, or instability, of certain fluid motions. *Proc. London Math. Soc.* **11**: 57–72.
Rey FA, Heinz FX, Mandl C, Kunz C, Harrison SC. 1995. The envelope glycoprotein from tick-borne encephalitis virus at 2 A resolution. *Nature* **375**: 291–298.
Roduit C, Saha B, Alonso-Sarduy L, Volterra A, Dietler G, Kasas S. 2012. OpenFovea: open-source AFM data processing software. *Nat. Methods* **9**:774–775.
Sandal M, Valle F, Tessari I, Mammi S, Bergantino E, Musiani F, Brucale M, Bubacco L, Samori B. 2008. Conformational equilibria in monomeric alpha-synuclein at the single molecule level. *PLoS Biol.* **6**: 0099–0108.
Sandal M, Benedetti F, Brucale M, Gomez-Casado A, Samorì B. 2009. Hooke: an open software platform for force spectroscopy. *Bioinformatics* **25**: 1428–1430.
Sekatskii SK, Favre M, Dietler G, Mikhailov AG, Klinov DV, Lukash SV, Deyev SM. 2010. Force spectroscopy of barnase–barstar single molecule interaction. *J. Mol. Recognit.* **23**: 583–588.
Sekatskii SK, Benedetti F, Dietler G. 2013. Dependence of the most probable and average bond rupture force on the force loading rate: first order correction to the Bell–Evans model. *J. Appl. Phys.* **114**: 034701.
Sorokin AV, Mikhailov AM, Kachko AV, Protopopova EV, Konovalova SN, Andrianova ME, Netesov SV, Kornev AN, Loktev VB. 2000. Human recombinant laminin binding protein: isolation, purification and crystallization. *Biochem. (Moscow).* **65**: 546–553.
Stiasny K, Bressanelli S, Lepault J, Rey FA, Heinz FX. 2004. Characterization of a membrane-associated trimeric low-pH-induced form of the class II viral fusion protein E from tick-borne encephalitis virus and its crystallization. *J. Virol.* **78**: 3178–3183.
Stiasny K, Fritz R, Pangerl K, Heinz FX. 2011. Molecular mechanisms of flaviviral membrane fusion. *Amino Acids* **41**: 1159–1163.
Stiasny K, Heinz FX. 2006. Flavivirus membrane fusion. *J. Gen. Virol.* **87**: 2755–2766.
Strauss JH, Wang KS, Schmaljohn AL, Kuhn RJ, Strauss EG. 1994. Host-cell receptors for Sindbis virus. *Arch. Virol. Suppl.* **9**: 473–484.
Ternovoi VA, Protopopova EV, Chausov EV, Novikov DV, Leonova GN, Netesov SV, Loktev VB. 2007. Novel variant of tickborne encephalitis virus. *Russia. Emerg. Infect. Dis.* **13**: 1574–1578.
van der Most RG, Corver J, Strauss JH. 1999. Mutagenesis of the RGD motif in the yellow fever virus 17D envelope protein. *Virology* **265**: 83–95.
Weisel JW, Shuman H, Litvinov RI. 2003. Protein–protein unbinding induced by force: single-molecule studies. *Curr. Opin. Struct. Biol.* **13**: 227–235.
Zhang WK. 2011. AFM imaging and single molecule force spectroscopy studies on macromolecular interactions at single molecule level. *Acta Polymer. Cinica.* **9**: 913–920.
Zuber C, Knackmuss S, Rey C, Reusch U, Röttgen P, Fröhlich T, Arnold GJ, Pace C, Mitteregger G, Kretzschmar HA, Little M, Weiss S. 2008. Single chain Fv antibodies directed against the 37 kDa/67 kDa laminin receptor as therapeutic tools in prion diseases. *Mol. Immunol.* **45**: 144–151.